Phosphorylation of Myosin Regulatory Light Chain Eliminates Force-Dependent Changes in Relaxation Rates in Skeletal Muscle

Jitandra R. Patel, Gary M. Diffee, Xu Pei Huang, and Richard L. Moss
Department of Physiology, University of Wisconsin, Madison, Wisconsin 53706 USA

ABSTRACT The rate of relaxation from steady-state force in rabbit psoas fiber bundles was examined before and after phosphorylation of myosin regulatory light chain (RLC). Relaxation was initiated using diazo-2, a photolabile Ca^{2+} chelator that has low Ca^{2+} binding affinity ($K_{Ca} = 4.5 \times 10^5\ M^{-1}$) before photolysis and high affinity ($K_{Ca} = 1.3 \times 10^7\ M^{-1}$) after photolysis. Before phosphorylating RLC, the half-times for relaxation initiated from 0.27 ± 0.02, 0.51 ± 0.03, and 0.61 ± 0.03 P_o were 90 ± 6, 140 ± 6, and 182 ± 9 ms, respectively. After phosphorylation of RLC, the half-times for relaxation from 0.36 ± 0.03 P_o, 0.59 ± 0.03 P_o, and 0.65 ± 0.02 P_o were 197 ± 35 ms, 184 ± 35 ms, and 179 ± 22 ms. This slowing of relaxation rates from steady-state forces less than 0.50 P_o was also observed when bundles of fibers were bathed with *N*-ethylmaleimide-modified myosin S-1, a strongly binding cross-bridge derivative of S1. These results suggest that phosphorylation of RLC slows relaxation, most likely by slowing the apparent rate of transition of cross-bridges from strongly bound (force-generating) to weakly bound (non-force-generating) states, and reduces or eliminates Ca^{2+} and cross-bridge activation-dependent changes in relaxation rates.

INTRODUCTION

Myosin regulatory light chain (RLC) of vertebrate striated muscle is predominantly bound to the myosin head, i.e., to subfragment 1 (S1), although its amino-terminal domain extends onto the rodlike subfragment 2 (Winkelman and Lowey, 1986; Rayment et al., 1993). Myosin RLC is phosphorylated by Ca^{2+}-calmodulin-dependent myosin light chain kinase, and in vertebrate striated muscle this phosphorylation has been associated with a potentiation of twitch force and an increased rate of rise of force (reviewed by Sweeney et al., 1993). In intact skeletal muscle, both posttetanic twitch potentiation (Barany and Barany, 1977; Manning and Stull, 1982), a transient increase in twitch amplitude subsequent to a brief tetanic contraction, and treppe (Klug et al., 1982), a progressive increase in the amplitude of successive closely spaced twitches, correlate well with the amount of phosphate incorporated into RLC. A causal relationship between measured force and increased phosphorylation of RLC was subsequently shown in skinned skeletal muscle fibers (Metzger et al., 1989; Sweeney and Stull, 1990). The increase in submaximum force was accompanied by a faster rate of rise of submaximum force in skinned skeletal fibers, suggesting that phosphorylation of RLC also plays a role in determining the kinetics of cross-bridge interaction. Partial extraction of RLC has been shown to increase the rate of force development in skeletal muscle (Patel et al., 1996), whereas replacement of endogenous RLC with a nondivalent cation-binding mutant RLC slowed the rate of force development (Diffee et al., 1996), indicating that the RLC has an important role in determining the rate of force development.

Although there has been much recent work examining the process of force development in striated muscles, relaxation from steady state-force after cessation of stimulation remains a poorly understood process. For example, relaxation of isometric force after tetanus in skeletal muscle occurs in two phases: an initial linear phase, which is characterized by uniformity of sarcomere length along the fiber, and a second phase that is more or less exponential, in which some regions of the fibers shorten and other regions elongate (Huxley and Simmons, 1970; Edman and Flitney, 1982). However, the cellular mechanisms underlying these distinct phases are not understood. Studies of relaxation in tetanized intact fibers are complicated by the process of Ca^{2+} diffusion and Ca^{2+} reuptake by the sarcoplasmic reticulum upon the cessation of stimulation. The use of photolabile Ca^{2+} chelators has made it possible to focus on the process of force relaxation at the myofilament level. Diazo-2, a Ca^{2+} chelator that rapidly binds Ca^{2+} when exposed to a flash of UV light (Adams et al., 1989), has been used to study relaxation in single skeletal muscle fibers from frog (Wahr and Rall, 1996), as well as in skinned smooth (Khromov et al., 1995) and cardiac (Zhang et al., 1995; Palmer and Kentish, 1997) muscles.

Given the importance of the RLC and RLC phosphorylation in modulating force development kinetics, we examined the role of RLC phosphorylation in determining the rate of relaxation from steady-state force after flash photolysis of diazo-2. The results of this study indicate that in skeletal muscle, the rate of relaxation varies inversely with the level of activation, and this activation dependence of relaxation rate is eliminated by phosphorylation of RLC. Furthermore, relaxation from low levels of steady-state force was slower in the presence than in the absence of phosphorylated RLC. *N*-ethylmaleimide-modified myosin

Received for publication 12 June 1997 and in final form 21 October 1997.

Address reprint requests to Dr. Jitandra R. Patel, Department of Physiology, University of Wisconsin, School of Medicine, 1300 University Avenue, Madison, WI 53706. Tel.: 608-262-0694; Fax: 608-265-5512; E-mail: patel@facstaff.wisc.edu.

0006-3495/98/01/360/09 $2.00

S-1 (NEM-S1), a strongly binding derivative of S-1, had effects on relaxation similar to those due to phosphorylation of RLC. These findings suggest that phosphorylated RLC slows the transition of cross-bridges from strongly bound (force-generating) to weakly bound (non-force-generating) states.

MATERIALS AND METHODS

Experimental solution, apparatus, and protocol

The compositions of experimental solutions used in the present study are shown in Table 1. Rabbit psoas fibers were skinned by a method described earlier (Patel et al., 1996). On the day of an experiment, a bundle of skinned psoas fibers was transferred to relaxing solution and cut into segments that were ~3 mm long. The segments were then split into smaller bundles of three or four fibers, and one of these bundles was transferred to relaxing solution in a stainless steel experimental chamber assembly similar to one described previously (Moss et al., 1983). The ends of the fiber bundle were attached to the arms of a motor (model 350; Cambridge Technology, Cambridge, MA) and a force transducer (model 403; Cambridge Technology), as described by Moss et al. (1983). The stainless steel chamber assembly was then placed on the stage of an inverted microscope (Olympus) fitted with a 40× objective and a video camera (model WV-BL600; Panasonic). Light from a halogen lamp on the microscope was passed through a cutoff filter (transmission >620 nm) and was then used to illuminate the fiber bundle. Using this filtered light, it was possible to record and store video images of each fiber bundle before, during, and after photolysis of diazo-2 with UV light (300–360 nm) generated from a xenon flash lamp (Hi-Tech Scientific, Salisbury, England). These video images were used to assess mean sarcomere length (SL) during the course of the experiment. Changes in force were recorded on a chart recorder (Allen Datagraph) on a slow time scale and with an oscilloscope (Nicolet 310) on a faster time scale.

Once the temperature (15°C) of the stainless steel chamber assembly was stabilized, the fiber bundle was stretched to a SL of 2.45 μm. To determine the Ca^{2+} dependence of steady-state force, the fiber bundle was first transferred from relaxing solution to low-EGTA preactivating solution (2 min), and then from preactivating to a range of activating solutions (pCa 4.5, 6.0, 6.1, 6.2). Once the force reached steady state, the fiber bundle was rapidly slackened to record an accurate force baseline and was then transferred back to relaxing solution. Fig. 1 shows the experimental protocol used to record relaxation of the fiber bundle from steady-state force subsequent to flash photolysis of diazo-2 (Molecular Probes). The fiber bundle was first incubated for 4 min (2 × solution change) in preactivating solution, then in loading solution containing diazo-2 and 0.1–0.6 mM $CaCl_2$ for 2 min, and finally in silicone oil. While the bundle was in oil, diazo-2 was photolyzed within the fiber bundle by a single, maximum intensity flash of UV light from a flash lamp. After the relaxation transient was recorded, the fiber bundle was transferred back to relaxing solution. The ability of the fiber bundle to generate steady-state force at pCa 4.5 was reexamined to determine whether significant fiber rundown had occurred. At the end of the experiment, the fiber bundle was cut free at the points of attachment and stored in sodium dodecyl sulfate sample buffer for subsequent protein analysis by sodium dodecyl sulfate-polyacrylamide gel electrophoresis.

TABLE 1 Composition of experimental solutions (mM)

Solution	EGTA	$CaCl_2$	$MgCl_2$	ATP	K-propionate
pCa 9.0 (relaxing)	7.00	0.02	5.42	4.73	59.71
Preactivating	0.07	—	5.27	4.76	70.45
pCa 4.5	7.00	7.01	5.27	4.82	37.49
Loading	—	0.10–0.60	5.99	4.75	77.85

In addition, all solutions contained (mM): 100.0 BES, 14.5 creatine phosphate, and 5.0 dithiothreitol. Loading solution also contained 100 units creatine kinase/ml and 2 mM diazo-2. pCa 6.2–6.0 was made by mixing a solution of pCa 9.0 and pCa 4.5 solution. The pH of all the solutions was adjusted to 7.0 at 15°C with KOH. The apparent stability constant used for Ca-EGTA was 2.391×10^6 M^{-1} at 15°C and pH 7.0. The computer program of Fabiato (1988) and apparent stability constants listed by Godt and Lindley (1982) were used to calculate the final concentration of each metal, ligand, and metal-ligand complex.

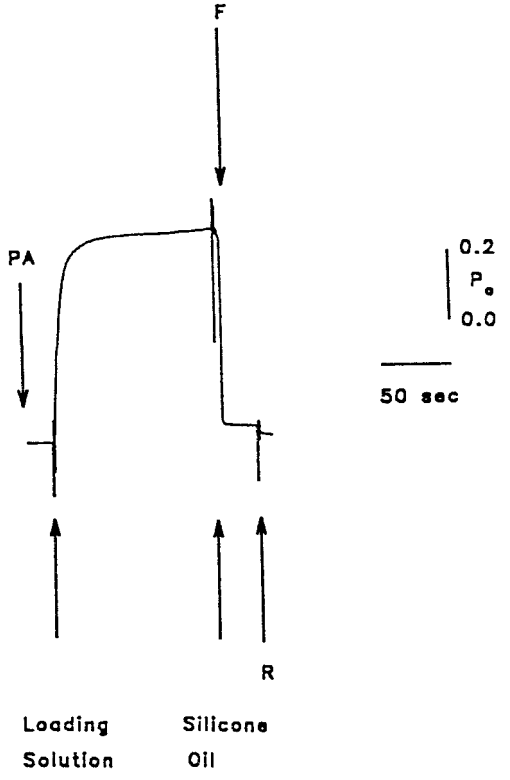

FIGURE 1 Experimental protocol for recording relaxation of rabbit psoas fiber bundles from steady-state force, initiated by flash photolysis of diazo-2. After the maximum force (P_o) generated at pCa 4.5 was recorded, the fiber bundle was incubated in preactivating solution (PA) for 4 min (only the last 20 s of incubation time is shown here) and was then transferred first to loading solution containing 0.3 mM $CaCl_2$ and 2 mM diazo-2 (2 min), and finally to silicone oil. While in silicone oil, the bundle was exposed to a maximum intensity flash (F) of UV light. After flash photolysis of diazo-2, the force was allowed to reach a new steady state before the fiber bundle was transferred to relaxing solution (R).

In the primary experiments, we investigated the effect of phosphorylation of RLC on both the steady-state force and the rate of relaxation from steady force initiated by flash photolysis of diazo-2. The experimental protocol was the same as above, except that RLC was phosphorylated after steady-state force was initially recorded at pCa 4.5, 6.1, and 6.0, and the effects of phosphorylation on both the steady-state force and the rate of relaxation from steady-state force were then examined.

To phosphorylate RLC, the fiber bundle was first incubated for 10 min in relaxing solution containing 6 μM calmodulin (CalBiochem) and 0.5 μM myosin light-chain kinase. The fiber bundle was then transferred five times between this solution (2 min) and an identical solution (45 s) containing 0.03 mM $CaCl_2$ and no EGTA. Myosin light-chain kinase used for phosphophorylating RLC was extracted and purified from rabbit fast skeletal muscle by the method of Nagamoto and Yagi (1984), with the modifications described by Metzger et al. (1989).

In another set of experiments, we investigated the effect of *N*-ethylmalemide-modified myosin S-1 (NEM-S1) on both the steady-state force and the rate of relaxation from steady-state force subsequent to flash photolysis of diazo-2. The experimental protocol was similar to the one described above, except that the fiber bundle was not treated with calmod-

ulin and kinase, and instead was bathed in relaxing solution containing NEM-S1, prepared by the methods of Williams et al. (1988) and Watterson et al. (1975) (i.e., there was no phosphorylation of RLC). Each fiber bundle was bathed in relaxing solution containing 6 mg NEM-S1/ml for 20 min, and the level of incorporation of NEM-S1 was maintained nearly constant by including 6 mg NEM-S1/ml in the preactivating and loading solutions.

Data analysis

The steady-state forces (P) generated by the fiber bundles in solution pCa 6.0–6.2 and in loading solution containing 2 mM diazo-2 and 0.1–0.6 mM $CaCl_2$ were expressed as fractions of the maximum force (P_o) generated by the same fiber bundle at pCa 4.5 at the start of an experiment.

Phosphorylation of RLC in the psoas fiber bundles was verified by isoelectric focusing (Metzger et al., 1989).

The time course of relaxation initiated by flash photolysis of diazo-2 was resolved into two distinct phases: an initial linear phase followed by a double exponential phase, as illustrated in Fig. 2. Four variables were assessed for quantitative analysis of relaxation kinetics: the half-time of relaxation (the time for the steady-state force to decrease by 50% after photolysis of diazo-2), the slope of the linear phase, and rate constants (k_1 and k_2) derived from the double-exponential phase. The transition between the linear phase and the double-exponential phase was determined in two ways. First, the entire relaxation transient was fit at 10-ms intervals with a double-exponential decay equation, $y = a*\exp(-k_1*x) + b*\exp(-k_2*x) + c$, where a and b are the amplitudes of the first and second phases, respectively, and c is the residual amplitude. The transition point determined from this fit was similar to the one determined by the second method (Khromov et al., 1995), in which d(normalized force)/dt was plotted against time.

Statistical analysis of the data was done using a paired t-test when data were acquired from the same fiber bundle, and unpaired t-tests when data were acquired from different fiber bundles. A p value of <0.05 was taken as indicating significant differences.

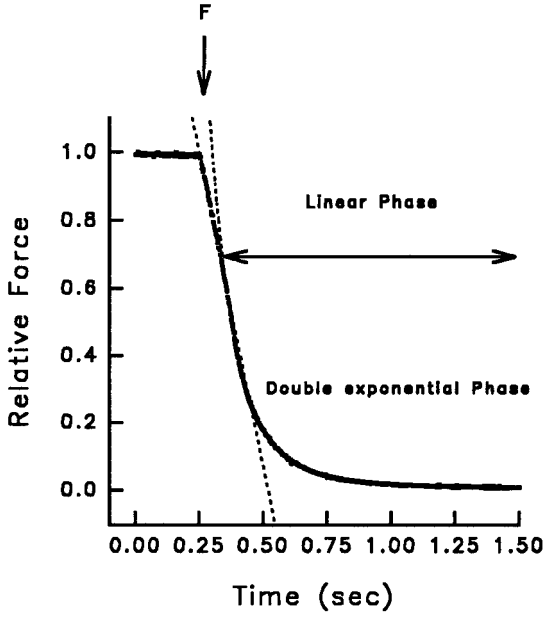

FIGURE 2 Two phases of relaxation from steady-state force after flash photolysis of diazo-2. The data in Fig. 1 are replotted on a faster time base to illustrate the two phases of the relaxation transient. Dashed lines represent the linear and the extrapolated double-exponential fits to experimental data points (*points*). The fit lines were extrapolated beyond prephotolysis steady-state force to clearly illustrate the two phases of the relaxation transient. Relaxation properties: half-time of relaxation = 132 ms; slope = 3.72 s^{-1}; k_1 = 8.99 s^{-1}; k_2 = 1.87 s^{-1}.

RESULTS

Activation dependence of relaxation rate

Fig. 3 *A* shows time courses of force relaxation from different levels of activation when similar amounts of diazo-2 were photolyzed within bundles of psoas fibers. Before photolysis, the steady-state forces generated by this fiber bundle in loading solutions containing 2 mM diazo-2 and 0.2, 0.3, and 0.4 mM total $CaCl_2$ were 0.27 P_o, 0.50 P_o, and 0.60 P_o, respectively. Relaxation from forces greater than ~0.60 P_o were not systematically studied because photolysis of diazo-2 did not fully relax force. After photolysis of diazo-2, there was a 90% or greater decrease in steady-state force due to rapid Ca^{2+} chelation by diazo-2. Half-times for relaxation increased from 100 to 200 ms as the pre-flash levels of activation were increased from 0.27 to 0.60 P_o. To

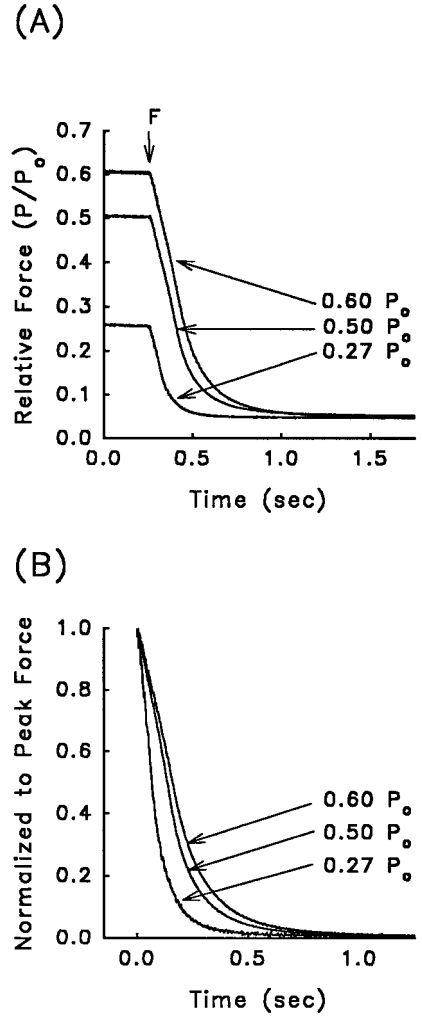

FIGURE 3 Activation-dependent changes in relaxation rate in skinned psoas fiber bundles. (*A*) Relaxation initiated by photolysis of diazo-2 (F) from three different levels of activation, achieved by incubating the fiber bundles in loading solution containing 2 mM diazo and 0.2 (0.27 P_o), 0.3 (0.50 P_o), and 0.4 (0.60 P_o) mM $CaCl_2$. Force is expressed relative to maximum force generated by the fiber bundles when incubated in pCa 4.5 solution. (*B*) The relaxation transients in *A* were replotted after normalizing to peak amplitude of steady-state force before flash photolysis.

quantify the activation-dependent changes in relaxation rates, the same data were expressed relative to peak steady-state force developed by the fiber bundle before photolysis and replotted (Fig. 3 *B*). It can be seen that relaxation takes longer when initiated from higher levels than at lower levels of steady-state force. Similar data from several fiber bundles are summarized in Fig. 4. In addition, the slope of the linear phase of relaxation (Fig. 4 *B*) and both k_1 (Fig. 4 *C*) and k_2 (Fig. 4 *D*) of the double-exponential phase of relaxation decreased as preflash steady-state force was increased. However, the fractional amplitudes of the linear phase and the two components of the exponential phase of relaxation did not change greatly with the level of activation (Table 2).

Effects of RLC phosphorylation on activation-dependent changes in relaxation rates

We examined the effects of RLC phosphorylation on both steady-state force and on the time course of relaxation from various steady-state forces developed by incubating the fiber bundles in loading solution containing 2 mM diazo-2 and 0.15, 0.30, or 0.40 mM $CaCl_2$. The steady-state forces developed by the fiber bundles ($n = 13$) at pCa 6.1 and 6.0 were 0.23 ± 0.02 and 0.53 ± 0.01 P_o, respectively, before phosphorylation, and 0.31 ± 0.02 and 0.53 ± 0.01 P_o after phosphorylation. The only statistically significant difference in force due to phosphorylation was at pCa 6.1. After phosphorylation of RLC, the steady-state forces in loading solution containing 2 mM diazo-2 and 0.15, 0.3, and 0.4 mM $CaCl_2$ were 0.36 ± 0.03 P_o ($n = 5$), 0.59 ± 0.03 P_o ($n = 4$), and 0.65 ± 0.02 P_o ($n = 4$), respectively (Fig. 5, *open circles*). Consistent with the results above, a significant increase in steady-state force was observed after phosphorylation only when the bundles were incubated in loading solution containing the lowest concentration of total Ca^{2+} tested. This increase in Ca^{2+}-activated force correlated well with increased phosphorylation of RLC (the ratio of RLC-P/(RLC + RLC-P) was 0.85 ± 0.10, $n = 6$)

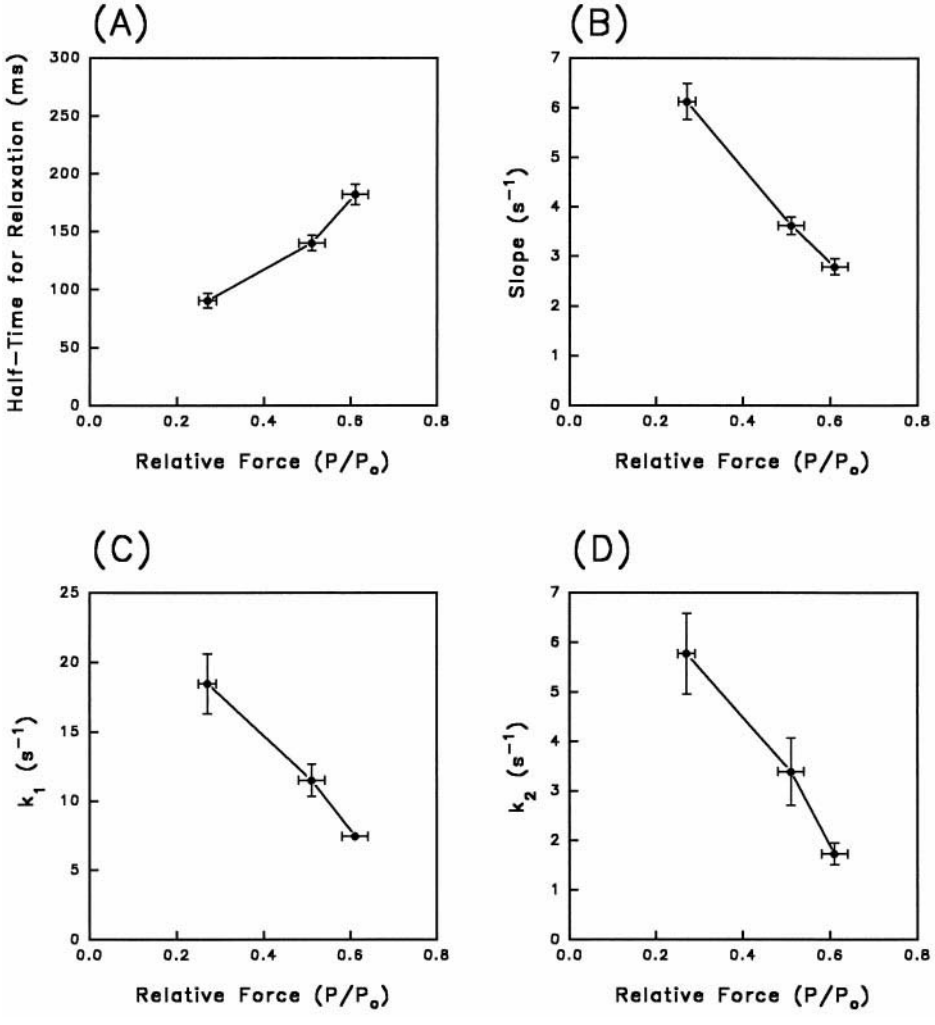

FIGURE 4 Amplitude-dependent changes in properties of the relaxation transients initiated by photolysis of diazo-2. Before photolysis of diazo-2, different levels of steady-state force were achieved by incubating the fiber bundles in loading solution containing 0.2, 0.3, and 0.4 mM $CaCl_2$. Summaries of relaxation properties are presented for all fiber bundles: (*A*) half-time of relaxation, (*B*) slope of the linear phase, (*C*) rate constant k_1 of the first amplitude, and (*D*) rate constant k_2 of the second amplitude of the double-exponential phase. Each data point represents the mean, and the error bars represent the SEM.

TABLE 2 Amplitudes of linear and double-exponential phases of the relaxation transients before and after phosphorylation of RLC and incorporation of NEM-S1

				Double-exponential phase		
n	$CaCl_2$ in loading solution (mM)	Steady-state force (P/P_o)	Linear phase	a	b	c
Amplitudes of relaxation transients in psoas fiber (control)						
7	0.20	0.27 ± 0.02	0.369 ± 0.018	0.436 ± 0.056	0.190 ± 0.051	0.005 ± 0.002
5	0.30	0.51 ± 0.03	0.348 ± 0.012	0.507 ± 0.046	0.141 ± 0.040	0.004 ± 0.001
4	0.40	0.61 ± 0.03	0.349 ± 0.011	0.570 ± 0.034	0.080 ± 0.026	0.001 ± 0.001
Amplitudes of relaxation transients after phosphorylation of RLC						
5	0.15	0.37 ± 0.03	0.296 ± 0.019	0.515 ± 0.032	0.193 ± 0.034	−0.004 ± 0.01
4	0.30	0.59 ± 0.03	0.329 ± 0.006	0.574 ± 0.018	0.093 ± 0.023	0.004 ± 0.001
4	0.40	0.65 ± 0.02	0.325 ± 0.01	0.539 ± 0.031	0.133 ± 0.031	0.003 ± 0.001
Amplitudes of relaxation transients after incorporation of NEM-S1						
4	0.1	0.28 ± 0.02	0.280 ± 0.031	0.659 ± 0.047	0.058 ± 0.018	0.003 ± 0.001
4	0.2	0.37 ± 0.03	0.353 ± 0.022	0.517 ± 0.027	0.127 ± 0.014	0.003 ± 0.001

The amplitudes are expressed relative to peak steady-state forces before flash photolysis of diazo-2. a is the amplitude of the first exponential phase that relaxes with a rate constant k_1; b is the amplitude of the second exponential phase that relaxes with a rate constant k_2; c is the residual amplitude.

observed in the isoelectric focusing gels of fiber bundles subjected to the phosphorylation protocol (Fig. 6).

Fig. 5 summarizes relaxation data from several experiments done under identical conditions before and after RLC phosphorylation. After phosphorylation, the half-time for relaxation increased at low levels of activation, so that there were no activation-dependent differences in this variable: half-times were 197 ± 35 ms at 0.36 ± 0.03 P_o ($n = 5$), 184 ± 35 ms at 0.59 ± 0.03 P_o ($n = 4$), and 179 ± 22 ms at 0.65 ± 0.02 P_o ($n = 4$). Consistent with this result, RLC phosphorylation also reduced the slope of the linear phase (Fig. 5 *B*) and the rate constants k_1 (Fig. 5 *C*) and k_2 (Fig. 5 *D*) of the double-exponential phase of relaxation at low levels of activation, thereby eliminating the activation dependence of relaxation rate. The relative amplitudes of the linear phase and the two components of the exponential phase changed little with the level of activation (Table 2).

Effects of *N*-ethymaleimide-modified S1 on steady-state force and relaxation parameters

Experiments were carried out to investigate whether an increase in the numbers of strongly bound cross-bridges could account for phosphorylation-dependent changes in relaxation rates. This was done by bathing fibers in solution containing NEM-S1, a strong binding derivative of myosin S1. The steady-state forces developed by fiber bundles were increased by NEM-S1: forces at pCa 6.2 and 6.1 were 0.03 ± 0.01 P_o ($n = 12$) and 0.27 ± 0.02 P_o ($n = 8$) before and 0.07 ± 0.01 P_o and 0.34 ± 0.02 P_o after treatment with NEM-S1. After treatment, the steady-state force developed by the fiber bundles was 0.28 ± 0.02 P_o ($n = 4$) in loading solution containing 0.1 mM $CaCl_2$ (which was similar to the force recorded in control fibers when exposed to loading solution containing 0.2 mM $CaCl_2$) and 0.54 ± 0.04 P_o ($n = 4$) in loading solution containing 0.2 mM $CaCl_2$ (a significant increase relative to control force recorded in an identical loading solution). The effects of NEM-S1 on steady-state force observed here are similar to those reported earlier by Swartz and Moss (1992).

Fig. 7 summarizes the relaxation data from several experiments conducted under identical conditions before and after treatment with NEM-S1. NEM-S1 significantly increased the half-time of relaxation from a force of 0.28 ± 02 P_o and eliminated the activation dependence of this variable (Fig. 7 *A*). Likewise, NEM-S1 reduced the slope of the linear phase (Fig. 7 *B*) and the rate constants k_1 (Fig. 7 *C*) and k_2 (Fig. 7 *D*) of the double-exponential phase of relaxation at the lowest level of activation investigated here. The fractional amplitudes of the linear phase and the two components of the exponential phase did not change significantly with level of activation or in the presence of NEM-S1, and were not significantly different from those recorded in control fiber bundles (Table 2). By comparing these data (Fig. 7, *open circles*) with control data (Fig. 7, *closed circles*), it is apparent that the NEM-S1 slows the rate of relaxation initiated from low levels of activation and eliminates the force-dependent changes in relaxation rate in skeletal muscle, effects that are similar to those induced by phosphorylation of RLC.

DISCUSSION

Time course of muscle relaxation

It has been known for some time that relaxation of isometric force in skeletal muscle occurs in two phases: an initial linear phase, which is characterized by uniformity of sarcomere length along the fiber, and a second phase that is more or less exponential, in which some regions of the fibers shorten at the expense of other regions that elongate (Huxley and Simmons, 1970; Edman and Flitney, 1982). In the present study, records of relaxation after photolysis of diazo-2 were somewhat more complicated than relaxation in living fibers. Because sarcomere length was not held constant during our experiments, it seems likely that changes in the striation pattern may have occurred during both the linear and the double-exponential phases of relaxation. Such changes in sarcomere pattern are likely to have a minimal impact on our interpretations of the data, for several rea-

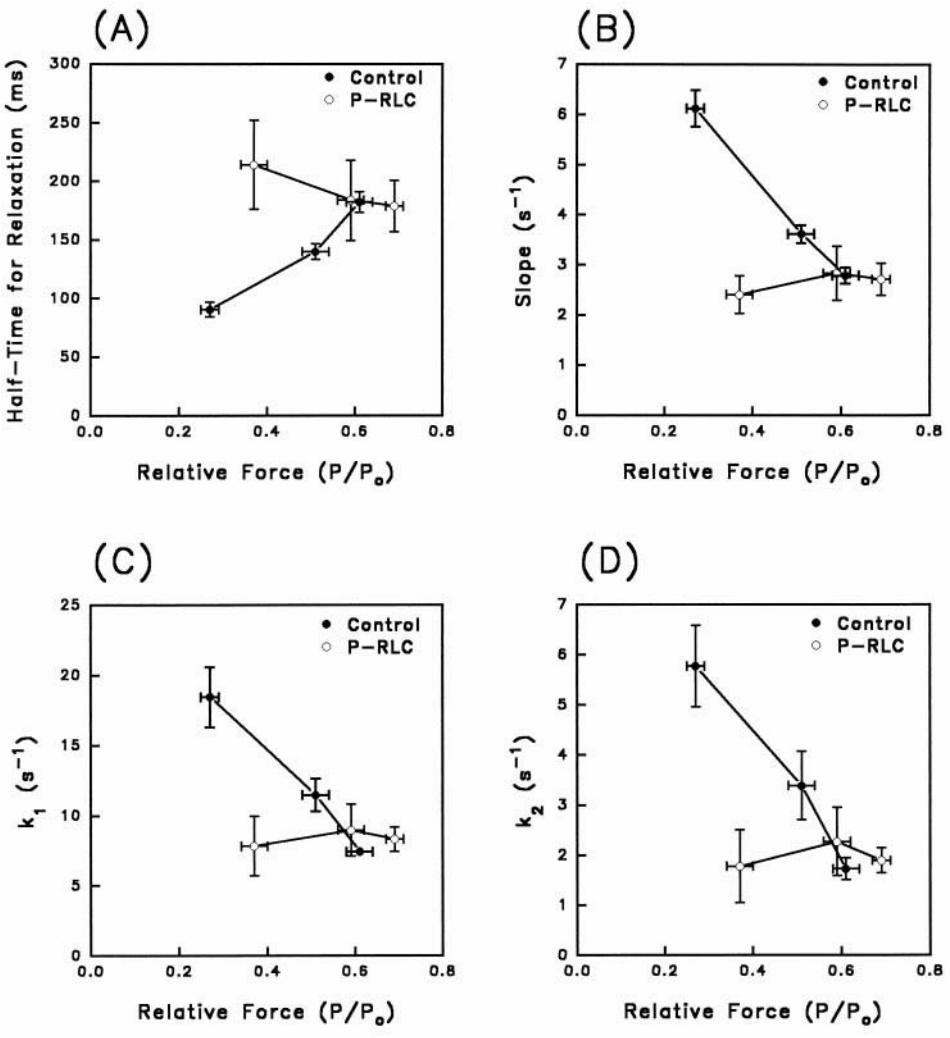

FIGURE 5 Effect of RLC phosphorylation on activation-dependent changes in relaxation properties. Before photolysis of diazo-2, different levels of steady-state force in RLC phosphorylated fiber bundles was achieved by incubating the bundles in loading solution containing 0.15, 0.3, and 0.4 mM $CaCl_2$. Summaries of relaxation properties are presented for all fiber bundles [before (●, data from Fig. 4) and after phosphorylation of RLC (○)]: (*A*) half-time of relaxation, (*B*) slope of the linear phase, (*C*) rate constant k_1 of the first amplitude, (*D*) rate constant k_2 of the second amplitude of the double-exponential phase. Each data point represents the mean, and the error bars represent the SEM.

sons. First, because control and test experiments were carried out under identical conditions, there would be similar changes in sarcomere pattern in the two sets of experiments. Second, Wahr and Rall (1996) showed that the two phases of relaxation in response to photolysis of diazo-2 were still evident in experiments in which attempts were made to control sarcomere length. Third, under all experimental conditions, the degree and direction of changes in the slope of the linear phase were similar to the changes observed in the double-exponential phase, suggesting that the processes underlying the linear phase are similar to those of the exponential phase.

Effects of activation levels on subsequent rates of relaxation

We have previously shown by photolysis of caged Ca^{2+} (DM-nitrophen) that the rate of force development in bundles of skinned psoas fibers increases with the level of activation (Patel et al., 1996). Activation dependence of k_{tr} was also evident when the rate of rise of force was assessed after rapid release and restretch of muscle fibers (Brenner, 1988; Metzger and Moss, 1992). In contrast to these earlier results, in the present study we have shown, by photolysis of diazo-2, that the rate of relaxation from steady-state force decreases with an increase in the level of activation. This effect of preflash force on rate of relaxation has been observed previously in single skeletal muscle fibers from frog (Wahr and Rall, 1996), but not in skinned smooth (Khromov et al., 1995) or cardiac (Zhang et al., 1995; Palmer and Kentish, 1997) muscles. These differences in results suggest that the force-dependent changes in relaxation rates observed here are skeletal muscle specific or that the relaxations from steady-state force in the earlier experiments on smooth and cardiac muscles (Zhang et al., 1995; Palmer and Kentish, 1997) may have been initiated when

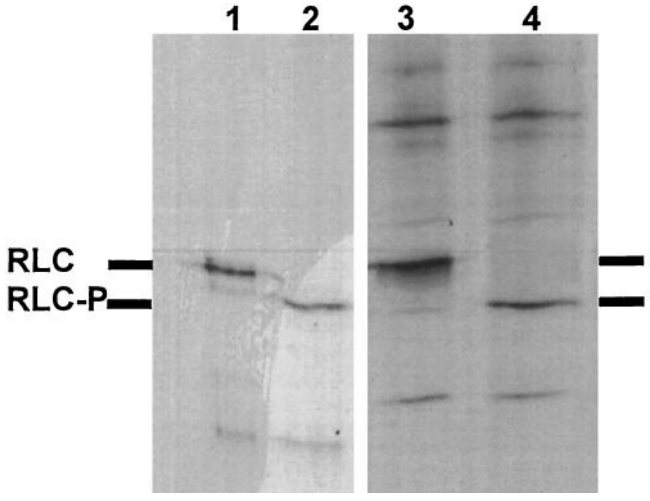

FIGURE 6 Isoelectric focusing gel of psoas fiber bundles. Lanes 1 and 2 contain samples of purified RLC without (*lane 1*) and after (*lane 2*) treatment with Ca^{2+}/calmodulin-dependent myosin light chain kinase. Lanes 3 and 4 contain samples of skinned fiber bundles before (*lane 3*) and after (*lane 4*) treatment to phosphorylate the RLC, as described in Materials and Methods (0.03 mM $CaCl_2$/6 μM calmodulin/0.5 μM myosin light chain kinase).

RLC was in a phosphorylated rather than in a dephosphorylated state. Although we have no data to definitively settle this point, we favor the latter explanation, because in the present study the amplitude-dependent changes in the rate of relaxation of skeletal muscle were eliminated by phosphorylation of RLC.

Basis for effects of phosphorylation on relaxation

At low concentrations of Ca^{2+}, the RLC phosphorylation-induced increase in steady-state force reported here and previously by Metzger et al. (1989) and Sweeney and Stull (1990) is likely to involve two factors: an increase in the rate of cross-bridge attachment and an increase in cooperative activation of the thin filament. As reviewed by Sweeney et al. (1993), RLC phosphorylation increases the rate of force development, which is most straightforwardly interpreted in terms of an increase in cross-bridge attachment rate. Moreover, disruption of thin filament long-range cooperativity by partial extraction of TnC eliminates RLC phosphorylation-induced increases in submaximum force (Metzger et al., 1989). In the present study, the similarity of effects on force due to NEM-S1 and phosphorylation of RLC further strengthens the idea that potentiation of force is due in part to increased cooperative activation of thin filaments by strong binding cross-bridges. Such a mechanism was suggested previously to explain the tendency of NEM-S1 to increase force at submaximum levels of activation (Swartz and Moss, 1992).

We also observed that the RLC phosphorylation-induced increase in steady-state force was accompanied by a decrease in the rate of subsequent relaxation. In contrast, previous studies found that the rate of rise of force was faster after phosphorylation of RLC (Metzger et al., 1989; Sweeney and Stull, 1990) or after incorporation of NEM-S1 into skeletal muscle fibers (Swartz and Moss, 1992). One possible explanation that would account for all of these changes in kinetics of contraction and relaxation is that both RLC phosphorylation and NEM-S1 enhance the level of activation of the myofilament. In NEM-S1 experiments, the increase in activation of the thin filaments is due to the binding of NEM-S1 to actin (Swartz and Moss, 1992), whereas the enhanced activation state in the RLC phosphorylation experiments is most likely a consequence of increased cross-bridge binding due to an increased probability of attachment, as proposed earlier (Metzger et al., 1989; Sweeney et al., 1993). Because such movement would predispose cross-bridges to attach to actin, force will develop more quickly when Ca^{2+} binds to the regulatory proteins on the thin filament. Once the cross-bridges are in a strongly bound, force-generating state, the predisposition of cross-bridges to attach, due to a high rate constant of attachment relative to detachment, will tend to keep the number of strongly bound cross-bridges high, even after Ca^{2+} is removed from the bathing solution. In this way, maintenance of cross-bridge-induced activation of the thin filament will slow the rate of relaxation. The fact that NEM-S1 had similar effects on the rate of relaxation strengthens the conclusion that increased cooperative activation of the thin filament by strongly bound cross-bridges is the basis for RLC phosphorylation-dependent effects on relaxation rate. In this regard, it appears that NEM-S1 and RLC phosphorylation might not be equally effective activators of the thin filament, because NEM-S1 eliminated the activation dependence of force development (Swartz and Moss, 1992), whereas RLC phosphorylation simply shifts the activation dependence to lower [Ca^{2+}] (Metzger et al., 1989; Sweeney and Stull, 1990). This difference may be more apparent than real, resulting straightforwardly from the larger number of NEM-S1 molecules as compared to endogenous cross-bridges with phosphorylated RLC. Alternatively, the greater effect of NEM-S1 could be due to the long-lived nature of its interaction with actin, as a manifestation of a very slow rate constant of detachment (e.g., Williams et al., 1988).

Both the NEM-S1-induced slowing of relaxation of skeletal muscle fibers observed here and the earlier report of inhibition of relaxation of native actomyosin preparations in the presence of NEM-modified myosin (Pemrick and Weber, 1975) suggest that after Ca^{2+} chelation, cross-bridges in the presence of NEM-S1 tend to remain for longer times in the force-generating state. This tendency of strongly bound cross-bridges to slow relaxation is consistent with the tendency of increased ADP concentration to slow relaxation from steady-state force initiated by photolyzing diazo-2 in frog skeletal muscle fibers (Ashley et al., 1990). In the presence of excess ADP, the active sites on myosin are largely populated by ADP, which is a strongly bound cross-bridge state (Schoenberg, 1988). Because the effect of RLC phosphorylation on relaxation rate was identical to that of NEM-S1, it is reasonable to conclude that after Ca^{2+} che-

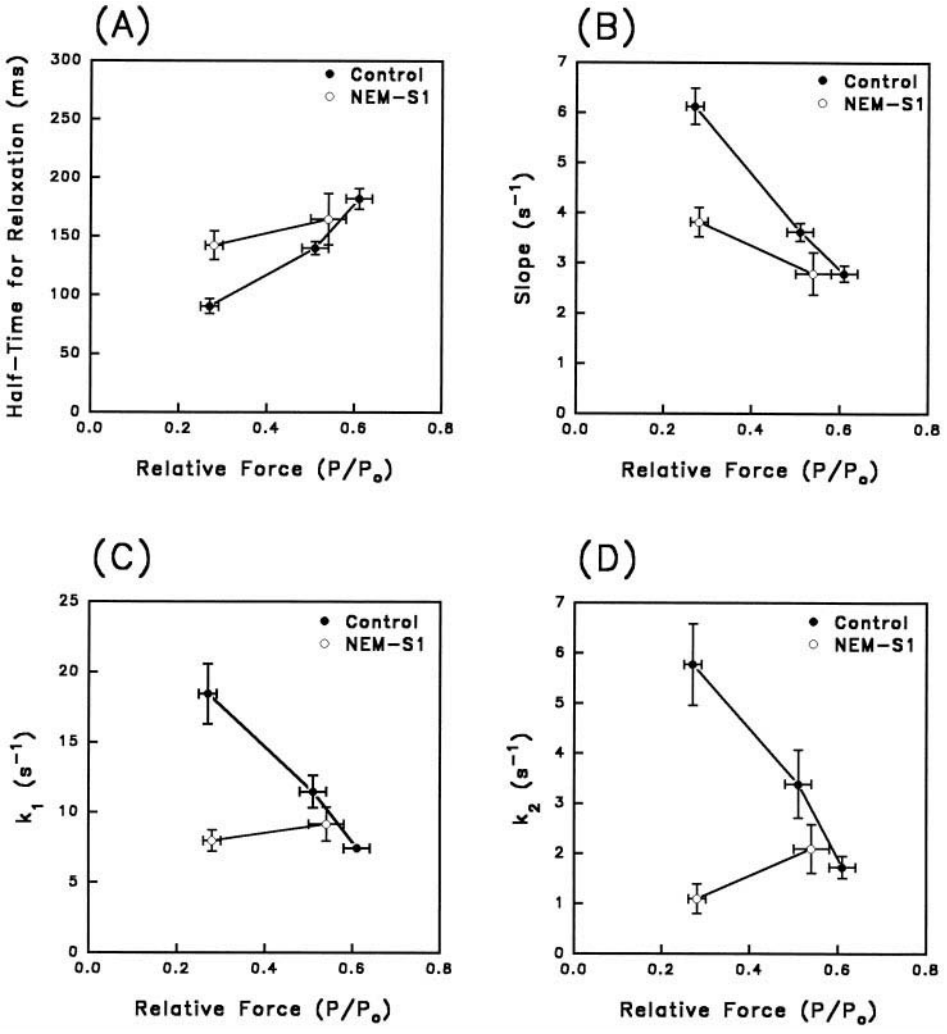

FIGURE 7 Effects of NEM-S1 on amplitude-dependent changes in relaxation properties. Before photolysis of diazo-2, different levels of steady-state force were achieved by incubating the NEM-S1-treated fiber bundles in loading solutions containing 0.1 and 0.2 mM $CaCl_2$. Summaries of relaxation properties are presented for all fiber bundles [in the absence (●, data from Fig. 4) and presence (○) of NEM-S1]: (*A*) half-time for relaxation, (*B*) slope of the linear phase, (*C*) rate constant k_1 for the first amplitude, (*D*) rate constant k_2 for the second amplitude of the double-exponential phase. Each data point represents the mean, and the error bars represent the SEM.

lation by photolysis of diazo-2, the phosphorylation-induced increase in strongly binding myosin heads continues to maintain the thin filament in an activated state for an extended duration.

In summary, the present results show that phosphorylation of RLC slows the rate of relaxation of skeletal muscle, presumably by slowing cross-bridge detachment. Further findings that NEM-S1, a strong binding cross-bridge derivative, had similar effects on relaxation suggest strongly that the phosphorylation-induced slowing of relaxation results from the prolonged cooperative activation of the thin filament, even after Ca^{2+} has been removed. We conclude that RLC phosphorylation is an important modulator of relaxation kinetics in skeletal muscle.

We thank Dr. J. Graham for IEF analysis of fiber bundles and Nadine Duchateau for preparing Ca^{2+}/calmodulin-dependent myosin light-chain kinase and NEM-S1.

This work was supported by a grant to RLM from the National Institutes of Health (HL47053).

REFERENCES

Adams, S. R., J. P. Y. Kao, and R. Y. Tsien. 1989. Biologically useful chelators that take up Ca^{2+} upon illumination. *Am. Chem. Soc.* 111: 7957–7968.

Ashley, C. C., I. P. Mulligan, and R. E. Palmer. 1990. ADP slows the relaxation of single permeabilized muscle fibers from frog following flash photolysis of the caged calcium-chelator, diazo-2. *J. Physiol. (Lond.).* 426:21P.

Barany, K., and M. Barany. 1977. Phosphorylation of the 18,000-dalton light chain of myosin during a single tetanus of frog muscle. *J. Biol. Chem.* 252:4752–4754.

Brenner, B. 1988. Effect of Ca^{2+} on cross-bridge turnover kinetics in skinned single rabbit psoas fibers: implications for regulation of muscle contraction. *Proc. Natl. Acad. Sci. USA.* 85:3265–3269.

Diffee, G. M., J. R. Patel, F. C. Reinach, M. L. Greaser, and R. L. Moss. 1996. Altered kinetics of contraction in skeletal muscle fibers containing

a mutant myosin regulatory light chain with reduced divalent cation binding. *Biophys. J.* 71:341–350.

Edman, K. A. P., and F. W. Flitney. 1982. Laser diffraction studies of sarcomere dynamics during "isometric" relaxation in isolated muscle fibers of the frog. *J. Physiol. (Lond.).* 329:1–20.

Fabiato, A. 1988. Computer programs for calculating total from specified free and free from specified total ionic concentrations in aqueous solutions containing multiple metals or ligands. *Methods Enzymol.* 157: 378–417.

Godt, R. E., and B. D. Lindley. 1982. Influence of temperature upon contractile activation and isometric force production in mechanically skinned muscle fibers of frog. *J. Gen. Physiol.* 80:279–297.

Huxley, A. F., and R. M. Simmons. 1970. Rapid "give" and the tension "shoulder" in the relaxation of frog muscle fibers. *J. Physiol. (Lond.).* 210:32P.

Khromov, A., A. V. Somlyo, D. R. Trentham, B. Zimmermann, and A. P. Somlyo. 1995. The role of MgADP in force maintenance by dephosphorylated cross-bridges in smooth muscle: a flash photolysis study. *Biophys. J.* 69:2611–2622.

Klug, G. A., B. R. Botterman, and J. T. Stull. 1982. The effect of low frequency stimulation on myosin light chain phosphorylation in skeletal muscle. *J. Biol. Chem.* 257:4688–4690.

Manning, D. R., and J. T. Stull. 1982. Myosin light chain phosphorylation-dephosphorylation in mammalian skeletal muscle. *Am. J. Physiol.* 242: C234–C241.

Metzger, J. M., M. L. Greaser, and R. L. Moss. 1989. Variation in cross-bridge attachment rate and tension with phosphorylation of myosin in mammalian skinned skeletal muscle fibers. *J. Gen. Physiol.* 93: 855–888.

Metzger, J. M., and R. L. Moss. 1992. Myosin light chain 2 modulates calcium-sensitive cross-bridge transitions in vertebrate skeletal muscle. *Biophys. J.* 63:460–468.

Moss, R. L., G. G. Giulian, and M. L. Greaser. 1983. Effects of EDTA treatment upon the protein subunit composition and mechanical properties of mammalian single skeletal muscle fibers. *J. Cell Biol.* 966: 970–978.

Nagamoto, H., and K. Yagi. 1984. Properties of myosin light chain kinase prepared from rabbit skeletal muscle by improved method. *J. Biochem.* 95:1119–1130.

Palmer, S., and J. C. Kentish. 1997. Differential effects of the Ca^{2+} sensitizers caffeine and CGP 48506 on the relaxation rate of rat skinned cardiac trabeculae. *Circ. Res.* 80:682–687.

Patel, J. R., G. M. Diffee, and R. L. Moss. 1996. Myosin regulatory light chain modulates the Ca^{2+} dependence of the kinetics of tension development in skeletal muscle fibers. *Biophys. J.* 70:2333–2340.

Pemrick, S., and A. Weber. 1975. Mechanism of inhibition of relaxation by *N*-ethylmalemide treatment of myosin. *Biochemistry.* 15:5193–5198.

Rayment, I., W. R. Rypniewski, K. Schimidt-Bäse, R. Smith, D. R. Tomchick, M. M. Benning, D. A. Winkelman, G. Wesenberg, and H. M. Holden. 1993. Three-dimensional structure of myosin subfragment-1: a molecular motor. *Science.* 261:50–58.

Schoenberg, M. 1988. The kinetics of weakly- and strongly-binding cross-bridges: implications for contraction and relaxation. *Adv. Exp. Biol. Med.* 266:189–202.

Swartz, D. R., and R. L. Moss. 1992. Influence of strong-binding myosin analogue on calcium-sensitive properties of skinned skeletal muscle fibers. *J. Biol. Chem.* 267:20497–20506.

Sweeney, H. L., B. F. Bowman, and J. T. Stull. 1993. Myosin light chain phosphorylation in vertebrate striated muscle: regulation and function. *Am. J. Physiol.* 264:C1085–C1095.

Sweeney, H. L., and J. Stull. 1990. Alteration of cross-bridge kinetics by myosin light chain phosphorylation in rabbit skeletal muscle: implications for the regulation of actin-myosin interaction. *Proc. Natl. Acad. Sci. USA.* 87:414–418.

Wahr, P. A., and J. A. Rall. 1996. Effects of striation stability and calcium on the rate of relaxation in skinned skeletal muscle fibers from the frog. *Biophys. J.* 70:A38.

Watterson, J. G., M. C. Schaub, R. Locher, S. Di Pierri, and M. Kutzer. 1975. Temperature-induced transition in the conformation of intermediates in the hydrolytic cycle of myosin. *Eur. J. Biochem.* 56:79–90.

Williams, D. L., L. E. Greene, and E. Eisenberg. 1988. Cooperative turning on of myosin S1 ATPase activity by the troponin-tropomyosin-actin complex. *Biochemistry.* 27:6987–6993.

Winkelman, D. A., and S. Lowey. 1986. Probing myosin head structure with monoclonal antibodies. *J. Mol. Biol.* 188:595–612.

Zhang, R., J. Zhao, A. Mandveno, and J. D. Potter. 1995. Cardiac troponin I phosphorylation increases the rate of cardiac muscle relaxation. *Circ. Res.* 76:1028–1035.